

Contents lists available at [SciVerse ScienceDirect](http://www.sciencedirect.com)

Journal of Archaeological Science

journal homepage: <http://www.elsevier.com/locate/jas>

Distilling zinc for the Ming Dynasty: the technology of large scale zinc production in Fengdu, southwest China

Wenli Zhou^{a,b,*}, Marcos Martín-Torres^a, Jianli Chen^b, Haiwang Liu^c, Yanxiang Li^d

^aUCL Institute of Archaeology, 31-34 Gordon Square, London WC1H 0PY, UK

^bSchool of Archaeology and Museology, Peking University, Beijing 100871, China

^cHenan Provincial Archaeology Institute, Zhengzhou 450000, China

^dInstitute of Historical Metallurgy and Materials, University of Science and Technology Beijing, Beijing 100083, China

ARTICLE INFO

Article history:

Received 15 June 2011

Received in revised form

5 October 2011

Accepted 21 October 2011

Keywords:

Zinc distillation

Retort

Coal

Brass

Mints

China

ABSTRACT

Our understanding of zinc distillation technology in ancient China has traditionally been limited by a lack of studies of production remains. The discovery of nearly 20 zinc smelting sites dated to the Ming Dynasty (AD 1368–1644) along the Yangtze River in Fengdu, Chongqing, southwest China since 2002 is allowing a detailed technological reconstruction of zinc production. This paper presents the analytical study by OM, SEM-EDS and EPMA-WDS of the production remains from three of these sites, including zinc ore, zinc metal, retorts and slag. The analytical results reveal the use of large-scale installations for zinc distillation with retorts made of pots, condensers, pockets and lids, all well designed to meet specific performance characteristics. The retorts were charged with iron-rich oxidic zinc ores, coal and charcoal; a high temperature of around 1200 °C and highly reducing atmosphere were achieved to reduce the zinc ores; the zinc vapour formed within the pots was cooled and collected in the condensers. The mass production of zinc in Fengdu was probably set up to supply governmental mints.

© 2011 Elsevier Ltd. All rights reserved.

1. Introduction

Zinc was one of the important metals in the ancient world, primarily as an essential component of the alloy brass. Brass was usually made by the cementation process, whereby metallic copper, zinc ores and charcoal were heated in crucibles and brass formed directly through the absorption of zinc vapour by the copper, rather than by alloying two liquid metals (Bayley, 1984, 1998; Martín-Torres and Rehren, 2002; Rehren, 1999a,b). This technique was required because of the extreme volatility of metallic zinc (it boils at 907 °C), which means zinc immediately volatilises when it forms from the ore (around 1000 °C), and it reoxidises as soon as it comes in contact with air. Thus complex reduction and condensation installations, rather than ordinary smelting furnaces, are necessary to produce metallic zinc.

Before Europe established large scale zinc production in the 18th century (Day, 1998; Dungworth and White, 2007), only India

and China produced unalloyed zinc on an industrial scale. Indian zinc production, based on the principle of distillation by descending, first appeared about 1000 years ago, boomed during the 14th to 16th centuries, and ceased in the early 19th century at Zawar, northwest India (Craddock et al., 1998). In contrast, the Chinese zinc smelting process was based on the principle of distillation by ascending, which seems fundamentally different from the Indian one. Chinese zinc was mainly used for making brass coins in the Ming and Qing dynasties (16th to 19th centuries); some was traded via European merchants to the world (Bonnin, 1924; Craddock and Hook, 1997; de Ruelle, 1995; Souza, 1991). Traditional zinc smelting processes were still in operation in southwest China until the late 20th century. They utilised mineral coal instead of charcoal, both as fuel and reducing agent.

Since the 1920s, a number of Chinese and British scholars have studied Chinese zinc smelting technology and its history, especially its inception, based on three sources of evidence: historical records (Zhang, 1925; Zhao, 1984; Zhou, 1993, 2001), scientific analyses of ancient brass coins (Bowman et al., 1989; Cowell et al., 1993; Dai and Zhou, 1992; Zhou and Fan, 1993) and field surveys of traditional zinc smelting processes (Hu and Han, 1984; Mei, 1990; Xu, 1998; Zhou, 1996; Craddock and Zhou, 2003). A major gap in our understanding of ancient Chinese zinc production, however, has been the lack of detailed technological reconstructions based on

* Corresponding author. UCL Institute of Archaeology, 31-34 Gordon Square, London WC1H 0PY, UK.

E-mail addresses: juliazhouw1@gmail.com (W. Zhou), m.martinon-torres@ucl.ac.uk (M. Martín-Torres), jianli_chen@pku.edu.cn (J. Chen), haiwangliu@yahoo.com.cn (H. Liu), liyanxiang@metall.ustb.edu.cn (Y. Li).

the study of ancient production remains. Recently excavated zinc production installations in Chongqing provide an excellent opportunity to address this issue (Liu et al., 2007).

2. Zinc smelting sites in Chongqing

Since 2002, about 20 zinc smelting sites have been found on banks of the Yangtze River in Fengdu county, Chongqing, southwest China (Fig. 1). They were all located on the first terraces of the banks at altitudes of 150–170 m. A peculiar type of large, sand-tempered pots with clear evidence of high temperature exposure was regarded as a diagnostic feature to identify these as zinc smelting sites. In addition, furnace foundations, minerals, zinc metal, slag and coal were also excavated at these sites.

Between 2001–2005, three contemporary sites, Miaobeihou, Puzihe and Muxiexi, were excavated by Henan Provincial Archaeology Institute. At Miaobeihou, several furnace foundations were identified but their shapes could not be reconstructed. Beside one of the furnace foundations, there was a series of vestiges composing a relative complete zinc smelting workshop, including a working shed, a working platform for crushing ore, a pit for crushing coal, a pit for charging the pots and a waste pit. The charging pit was previously mistaken for a round furnace foundation (Liu et al., 2007, 176). At Puzihe and Muxiexi, a few foundations of rectangular furnaces resembling the trough-shaped furnaces used in traditional zinc smelting were excavated. One relatively intact rectangular furnace at Puzihe (Fig. 2) is 15.2 m long and 1.3 m wide; over 40 brick bars were remaining on the foundation at intervals of 12–14 cm (Shanxi Provincial Archaeology Institute and Chongqing Municipal Bureau of Cultural Heritage, 2007).

Some smelting remains from Miaobeihou site were initially studied by Liu and colleagues (2007). They confirmed that the ceramic pots were used as retorts for zinc distillation and the site could be dated by radiocarbon dating to the 15th–17th centuries

AD, corresponding with the Ming Dynasty (AD 1368–1644). A preliminary technological reconstruction was made about the raw materials, structures of the furnaces and retorts, and the smelting process. The ceramic pot was identified as the main body of a retort, which would contain the raw materials. A cylindrical ceramic condenser was built on top of the rim of the pot. Inside the condenser there is a transversal ceramic partition, named pocket, with a hole on one side and a concave upper surface where the zinc would be collected as it condensed. The opening of the condenser is covered by a disc-like lid made of iron (Fig. 3). However, more detailed scientific analyses of different types of production remains were necessary to reconstruct the zinc smelting technology in detail, potentially allowing the future mapping of temporal and regional variants. This paper aims to contribute a more thorough understanding of the zinc smelting technology in Fengdu, using Miaobeihou as the main case study. The different ceramic fabrics used to make different parts of the retorts have been characterised, their raw materials identified and the adaptation of formal and material properties to optimise performance characteristics assessed. The original charge, zinc products and metallurgical process taking place within the retorts have been established by analysing raw materials, zinc metal and metallurgical residues. Following the Miaobeihou case study, further smelting remains from the sites of Puzihe and Muxiexi have been also examined for comparative purposes. Based on archaeological evidence, analytical results and documents on traditional zinc smelting, the technology of zinc production in Fengdu has been reconstructed.

3. Methods

A wide range of metallurgical remains from Miaobeihou were selected for analysis, including possible ores, zinc metal, retorts and slag. Several samples were chosen from each category of materials in order to assess their internal variability. For comparison, a few

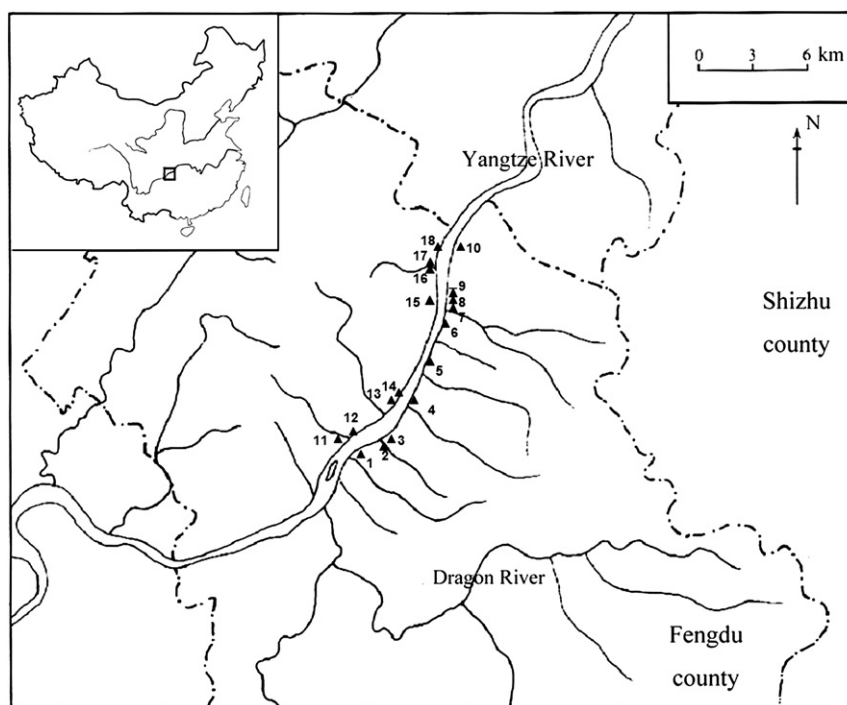


Fig. 1. Distribution map of zinc smelting sites in Fengdu. 1. Daoliuzi, 2. Miaobeihou, 3. Puzihe, 4. Muxiexi, 5. Shaxizui, 6. Qingjiayuan, 7. Yuanjiayan, 8. Shidiba, 9. Yuxi, 10. Hejiaba, 11. Jiudaoguai, 12. Langxi, 13. Chixi, 14. Qingquan, 15. Tingxi, 16. Hezuishang, 17. Tangfang, 18. Xiaoshuangxi. The Laochangping lead-zinc ore deposits in Shizhu lie 50 km southeast of these sites.

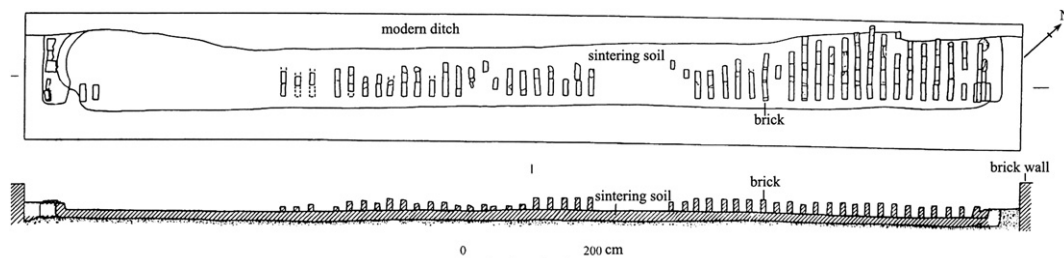


Fig. 2. Furnace Y2 at Puzihe site (modified after Shanxi Provincial Archaeology Institute and Chongqing Municipal Bureau of Cultural Heritage, 2007, 1762).

retort and slag samples from Puzihe and Muxiexi were also selected. Samples were named with three capital letters followed by a number. The first two letters refer to site (YM for Miaobeihou, CM for Muxiexi, YP for Puzihe); the third letter denotes the material type (O for ore, Z for zinc, B, M, T for bottom, middle and top parts of retorts respectively). The samples were mounted in epoxy resin and polished to 1 μm for optical microscopy (OM), scanning electron microscopy-energy dispersive spectrometry (SEM-EDS) and electron probe micro analysis-wavelength dispersive spectrometry (EPMA-WDS) examinations.

The OM used was a Leica DM LM. Microphotographs were taken at regular magnifications in plane polarised reflected light (PPL) and cross polarised reflected light (XPL).

The SEM used was a Philips XL30 environmental SEM with an Oxford Instruments INCA spectrometer package. The polished blocks were carbon coated. They were observed in secondary electron (SE) and backscattered electron (BSE) modes at regular magnifications, and analysed using the EDS system. The

acceleration voltage applied to all analyses was 20 kV, the working distance 10 mm, the spot size 5.0–5.6, the beam current adjusted to a deadtime of 35–40% and the livetime 50 s. Given the heterogeneous nature of most of the samples studied, the bulk compositions of the samples were obtained by averaging five measurements of large areas of ~ 2 by ~ 2.5 mm. Similarly, the ceramic matrices of the pots were analysed at areas of ~ 100 by ~ 150 μm , avoiding large inclusions; the glassy phases of the slag were studied at areas of ~ 400 by ~ 600 μm ; individual phases were probed by measuring spots of a few micrometres in diameter. Results were combined with oxygen by stoichiometry where appropriate. The accuracy of SEM-EDS decreases for values below 0.3%, but values below this threshold are reported for indicative purposes. Sodium was omitted in the analyses of samples rich in zinc (minerals, condensers, pockets and slag), because both Na $K\alpha$ and Na $K\beta$ peaks overlap with the Zn $L\alpha$ peak.

EPMA-WDS was employed to detect minor and trace elements in metallic zinc samples. The EPMA used is a JEOL JXA 8600 with an integrated operating system for the WDS analysis. The acceleration voltage applied was 20 kV, the beam current 5×10^{-8} A, the acquisition time 50 s. Three certified reference materials (41X4380Zn2, 41X0336Zn2, 41X0336Zn6) and three zinc samples were analysed at areas of ~ 80 by ~ 120 μm ten times. Three crystals were used: TAP (thallium acid phthalate) for the $L\alpha$ line of As; PET (pentaerythritol) for the $L\alpha$ lines of Sb, Sn, Ag and Cd, the $M\alpha$ lines of Pb and Bi, and the $L\beta$ line of In; LIF (lithium fluoride) for the $K\alpha$ lines of Zn, Fe and Cu. The nominal detection limits of these elements are about 0.03%, but again analytical results below these limits are presented.

4. Results

4.1. Minerals

Four mineral samples recovered from Miaobeihou site were analysed. YMO1-1, YMO1-2 and YMO2 are heavily weathered, porous, brick red mineral fragments with white or shiny minerals filling cavities. They are rich in ZnO (31–42%) and FeO (19–30%), and contain 5–6% SiO_2 , around 0.5% each CaO and MgO, and around 0.2% Al_2O_3 and CdO, with low analytical totals of 64–73%, consistent with the presence of carbonates and hydroxides which were not quantified by the EDS system (Table 1). They display finely intergrown oolitic structures of red minerals (iron oxides), and white minerals (zinc carbonates). The minerals growing in the cavities are zinc carbonates and zinc silicates. A fourth sample, YMO3, primarily consists of zinc silicates and quartz, so it is richer in SiO_2 (68.1%) and poorer in FeO (3.0%) (Table 1). These archaeological minerals were obviously not used by the ancient artisans, but given their high zinc contents, they may be cautiously considered as representative of the ores that could have been employed for zinc smelting.

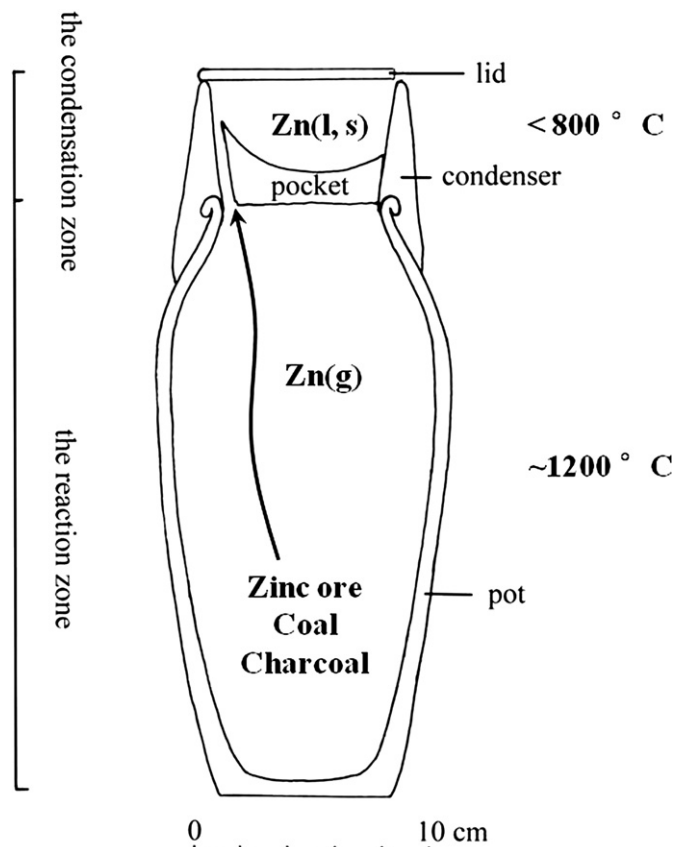


Fig. 3. Reconstruction of a retort (g-gas, l-liquid, s-solid).

Table 1

Average bulk compositions of mineral samples from Miaobeihou (wt%). Analyses on polished sections at areas of ~2 by ~2.5 mm by SEM-EDS. Both unnormalised (top half) and normalised (bottom half) results are presented. “—” means “not detected”.

Sample	MgO	Al ₂ O ₃	SiO ₂	Cl	CaO	FeO	ZnO	CdO	PbO	Total
YMO1-1	0.5	0.2	5.0	—	0.6	29.5	37.1	0.2	—	73.1
YMO1-2	0.7	—	6.4	—	0.4	19.4	42.4	0.3	—	69.6
YMO2	0.3	0.2	5.1	0.1	0.6	26.3	31.3	0.2	—	64.1
YMO3	0.3	0.8	68.1	0.1	0.5	3.0	32.9	0.1	0.1	105.9
YMO1-1	0.7	0.3	6.9	—	0.9	40.3	50.6	0.3	—	100.0
YMO1-2	1.0	—	8.4	—	0.6	28.4	61.2	0.4	—	100.0
YMO2	0.5	0.3	7.7	0.1	0.9	41.0	49.2	0.3	—	100.0
YMO3	0.3	0.8	63.5	0.1	0.5	3.1	31.5	0.1	0.1	100.0

4.2. Zinc

Over 10 zinc ingots were found by a local villager at Miaobeihou in the 1980s. He recalled that three of them were rectangular, at least 20 by 15 cm and about 5 cm thick; the others were plano-convex, less than 10 cm long and about 6 cm wide. The only surviving rectangular ingot (Fig. 4) was identified to be zinc of 99.2% purity (Liu et al., 2007).

Recent excavations at Miaobeihou discovered a few small amorphous lumps of metallic zinc. The three samples analysed are high purity metallic zinc with a few small lead-rich prills and euhedral intermetallic iron-zinc phases, FeZn₁₃. EPMA-WDS results confirmed that their main impurities are lead and iron (Table 2). YMZ1 and YMZ3 contain about half a percent of lead, while YMZ2 has less than 0.1% lead. Their iron contents are all below 0.1%. Other trace elements (arsenic, copper, silver, indium and cadmium) are below the detection limits (0.03%). The white patina on the surfaces is primarily composed of basic zinc carbonates and zinc sulphates. The outer parts contain earth minerals and coal fragments, which probably derive from the surrounding soils during burial.

4.3. Retorts

The retorts from the three sites share similar forms, consisting of four parts: pots, condensers, pockets and lids (Fig. 3). Analytical results of the ceramic pots, condensers and pockets from the three sites are presented as below.



Fig. 4. One of the zinc ingots discovered at Miaobeihou in the 1980s.

Table 2

Average compositions of zinc samples from Miaobeihou (wt%). Analyses on polished sections at areas of ~80 by ~120 μm by EPMA-WDS. “—” means “not detected”.

Sample	Zn	Fe	As	Cu	Ag	Pb	In	Bi	Cd	Total
YMZ1	98.08	0.05	0.01	0.01	—	0.41	0.01	0.01	0.01	98.59
YMZ2	98.99	0.02	—	—	0.01	0.06	0.01	—	0.01	99.10
YMZ3	98.41	0.04	—	—	—	0.42	0.01	0.01	0.01	98.90

4.3.1. Pots

The pots are wheel-thrown flat-bottomed jars, usually 25–30 cm in height (Fig. 5). Their flat bases are circular with diameters of 7–10 cm; the bodies open gradually to diameters of 11–16 cm and then close progressively; the rims are flared outwards with internal diameters of 6–9 cm. The pot bodies are about 0.6–1.0 cm thick and gradually become thinner from the bases to the rims. The colours of unused pots range from yellow, red and brown to grey due to variable firing conditions. The used pots are bluish grey, bluish black or black, indicating the strong reducing conditions required by zinc smelting (Fig. 5). Some used pots appear externally covered by a luting clay which is now highly vitrified and had coal ash fragments embedded, indicating that coal would have been the fuel employed to fire the furnaces.

Six pot samples from Miaobeihou, four from Muxiexi and four from Puzihe were analysed and found to have similar compositions and characteristics. The ceramic matrices are composed of 66–72% SiO₂, 19–24% Al₂O₃, 3–6% FeO and low levels of alkali and earth alkali oxides, their sum being about 4% (Table 3). The ZnO contents of most samples are around or below 0.3%, while only some of the used samples from Puzihe and Muxiexi, such as YPB5 and CMB4, contain just over 1%.

The fabrics of all the pot samples contain 10–15 vol% of large ill-sorted inclusions ranging from 50 μm up to 2 mm in diameter. They are sub-angular and show low sphericity. Most of the large inclusions are internally cracked quartz grains (Fig. 6), which are partially debonding from or dissolving into the surrounding ceramic. The internally cracked quartz grains are caused by the large thermal behaviour mismatch between the quartz grains and the surrounding glass phase, indicating a firing temperature of about 1200 °C (Ohya et al., 1999; Martín-Torres et al., 2008). A few molten feldspar grains, mostly potassium feldspar, are identified; some are totally molten, leaving only relict structures,



Fig. 5. Unused pot fragments collected from Miaobeihou in 2009 and a cross section of used pot fragment YMM9.

Table 3

Average matrix (top half) and bulk (bottom half) compositions of pot samples from three sites (wt%), normalised to 100%. Analyses on polished sections at areas of ~ 150 by ~ 200 μm and ~ 2 by ~ 2.5 mm respectively by SEM-EDS. YMM10, YMM13, YMM14, YPM1 and YPM4 are unused pots, while the others are used ones. “–” means “not detected”.

Site	Sample	Na ₂ O	MgO	Al ₂ O ₃	SiO ₂	P ₂ O ₅	SO ₃	Cl	K ₂ O	CaO	TiO ₂	MnO	FeO	ZnO
Miaobeihou	YMM1	0.4	0.6	19.1	72.3	0.1	–	–	2.1	0.3	0.9	–	4.2	–
	YMM3	0.3	0.7	20.1	70.7	0.1	–	–	3.1	0.1	1.0	–	3.9	–
	YMM9	0.2	0.8	22.1	67.0	0.1	–	–	2.7	0.2	1.1	–	5.8	–
	YMM10	0.2	0.7	21.6	68.1	0.2	–	–	2.7	0.2	1.0	–	5.3	–
	YMM13	0.3	0.7	23.6	65.9	0.2	–	–	2.8	0.2	1.0	–	5.3	–
	YMM14	0.2	0.7	21.9	69.9	0.1	–	0.1	3.0	0.2	0.8	–	3.0	0.1
Puzihe	YPM1	0.2	0.7	21.9	67.3	0.2	–	–	3.0	0.3	1.2	–	5.1	0.1
	YPM3	0.5	0.6	21.7	67.4	0.2	0.1	–	3.0	0.1	1.1	0.1	5.1	0.1
	YPM4	0.2	0.6	20.0	70.7	0.1	0.1	–	2.6	0.1	1.1	–	4.4	0.1
	YPB5	0.7	0.5	19.8	70.0	0.1	0.1	–	2.1	0.3	1.1	–	4.1	1.2
Muxiexi	CMT3	0.7	0.6	21.0	67.2	0.1	–	–	3.1	0.2	1.0	–	5.2	0.9
	CMM3	0.3	0.5	20.2	71.9	0.1	–	0.1	2.2	0.2	1.0	–	3.3	0.2
	CMB4	0.5	0.5	16.6	72.0	0.1	–	–	2.3	0.2	0.8	–	4.4	2.6
	CMB5	0.4	0.5	19.7	71.7	0.1	–	–	2.4	0.3	1.0	–	3.3	0.6
Miaobeihou	YMM1	0.3	0.5	14.8	77.7	0.2	–	–	1.7	0.3	0.8	–	3.6	0.1
	YMM3	0.2	0.7	17.3	73.8	0.1	–	–	2.8	–	0.9	–	4.1	0.1
	YMM9	0.2	0.6	18.7	69.9	0.1	0.1	–	2.4	0.2	1.0	–	6.8	–
	YMM10	0.1	0.6	18.2	71.3	0.1	0.1	–	2.4	0.2	0.9	–	6.0	0.1
	YMM13	0.2	0.5	18.4	72.1	0.1	–	–	2.2	0.3	0.8	0.1	5.3	–
	YMM14	0.1	0.5	16.8	76.5	0.2	0.1	0.1	2.3	0.1	0.7	–	2.5	0.1
Puzihe	YPM1	0.3	0.7	19.0	70.3	0.1	–	–	2.8	0.3	1.0	–	5.4	0.1
	YPM3	0.5	0.4	17.1	73.2	0.1	0.1	–	2.3	0.1	1.0	–	4.8	0.4
	YPM4	0.1	0.5	16.1	75.6	0.1	–	–	2.3	0.1	0.9	0.1	4.1	0.1
	YPB5	0.7	0.5	15.9	73.0	–	0.1	–	1.8	0.3	0.9	–	5.1	1.7
Muxiexi	CMT3	0.8	0.5	15.4	73.9	0.2	–	–	2.0	0.1	0.8	0.1	4.2	2.0
	CMM3	0.4	0.3	15.1	78.2	0.1	–	0.1	1.5	0.2	0.9	–	2.8	0.4
	CMB4	0.5	0.4	13.1	75.6	0.1	0.1	–	1.8	0.2	0.8	–	5.0	2.4
	CMB5	0.3	0.5	15.9	76.6	0.1	–	–	1.7	0.2	0.8	–	3.1	0.8

confirming that the firing temperature was over 1050 °C (Wolf, 2002). In unused samples, ferruginous concretions vary in size up to 2 mm in diameter; in used ones, most of the ferruginous concretions are molten and some iron-rich crystals have precipitated. In addition, smaller partially dissolved quartz grains are abundant in the matrices and are likely to have derived from the clay rather than being intentional temper. A few small inclusions, such as zircon, rutile and monazite, are also found in the fabrics.

The unused pots, mostly fired in a relatively oxidising atmosphere, show extensive vitrification of the ceramic matrices (Fig. 6). The used pots generally exhibit continuous vitrification structures with medium bloating pores (2–10 μm in diameter) (Fig. 7), which might be taken as an indication of the smelting temperature being higher than the original firing temperature by about 50–100 °C (cf. terminology in Maniatis and Tite, 1981; Tite et al., 1982). Nevertheless, the reducing atmosphere involved in zinc smelting usually

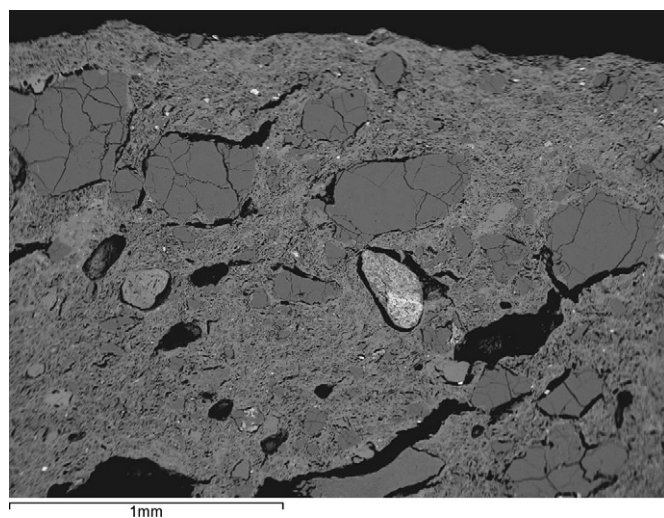


Fig. 6. BSE image of the cross section of the internal part of unused pot YMM14, showing the extensively vitrified matrix and inclusions of internally cracked quartz grains (dark grey) and ferruginous concretions (brighter grey).

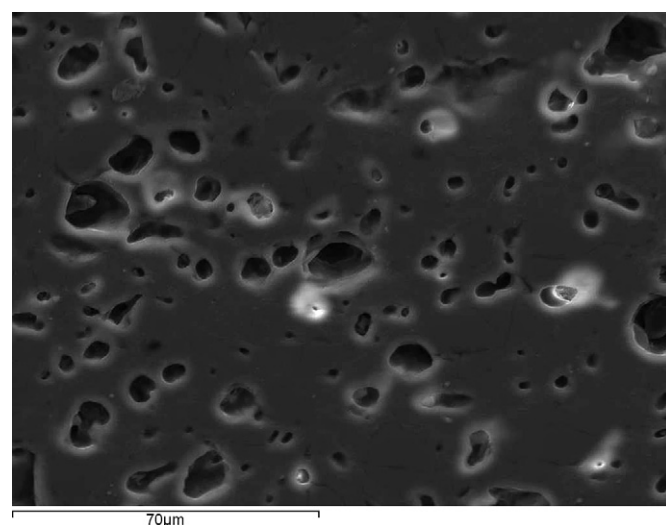


Fig. 7. SE image of the cross section of used pot YMM3, showing the continuous vitrification structure.

lowers the vitrification temperature by about 50 °C (Maniatis and Tite, 1981) and zinc contamination during use would flux the ceramic. Therefore, it can be inferred that the smelting temperature was similar to or slightly higher than the firing temperature of the pots, estimated at about 1200 °C. The bottom parts were sometimes exposed to a higher temperature as indicated by their larger bloating pores (10–50 µm in diameter).

4.3.2. Condensers

Cylindrical accessories of about 5 cm in height were built onto the rims of the pots, with the top ends thinner than the ends connected with the pots. They show a variety of colours ranging from yellow, brown and grey to black. Whitish or greenish substances adhere to the internal surfaces and the rims of condenser fragments, while only a limited amount of white deposits appear on the external surfaces. A few condenser fragments still preserve parts of pockets attached to their internal surfaces (Fig. 8).

In contrast with the pots, the condenser fabrics from the three sites show high levels of ZnO contamination, varying from 5% to 39%. To estimate the original compositions of the unused condensers, the ZnO contents were omitted, and the data renormalised to 100%. Compared to the pot fabrics, the condensers show more variable compositions, containing similar SiO₂ (64–75%), lower Al₂O₃ (13–18%), but higher levels of FeO (6–9%), K₂O (2–6%), CaO (1–3%) and MgO (1–2%). They also have slightly higher amounts of SO₃, P₂O₅ and Cl (Table 4).

These condenser fabrics contain over 30 vol% of ill-sorted inclusions. Most of them are angular quartz grains, ranging from 10 µm up to 500 µm large. There are also a significant number of

feldspar grains which show no evidence of thermal distortion. The most remarkable inclusions are fragments of coal ash, i.e. coal gangue minerals left after carbon was burnt out from coal. These fragments, usually with layered structures, vary in sizes, up to 2 mm long. A few coal ash fragments rich in carbon are also recognised due to their black colour under BSE imaging, low analytical totals and minor amounts of sulphur (Fig. 9). Three samples (YMT1, YMT3 and YMT17) contain higher proportions of coal ash fragments, resulting in their relatively higher contents of CaO. There are only small amounts of coal ash fragments in the other samples.

In some parts of the condensers, zinc-rich phases, mostly zinc oxides and carbonates, are deposited within the matrices and filling cracks. Even some mineral inclusions are heavily contaminated by zinc. The greenish and whitish crusts adhering to the condensers are mostly zinc oxides and zinc carbonates, with some post-depositional zinc sulphate and chloride minerals. A few droplets of metallic zinc with diameters of 50–500 µm are trapped within the crusts, in addition to a small number of siliceous minerals and coal (ash) fragments.

The upper parts of condensers are not vitrified, indicating that they were exposed to temperatures lower than 800 °C; the lower parts are highly vitrified with large bloating pores, the sizes of which increase from the rims of pots downwards (Fig. 10). Thus there were distinct temperature zones above and below the rims of pots. This would help keep the condensers relatively cool, thereby facilitating the condensation of the zinc vapour.

4.3.3. Pockets

Pockets are the concave horizontal ceramic dishes placed within the condensers where the metallic zinc collects. Rectangular holes,

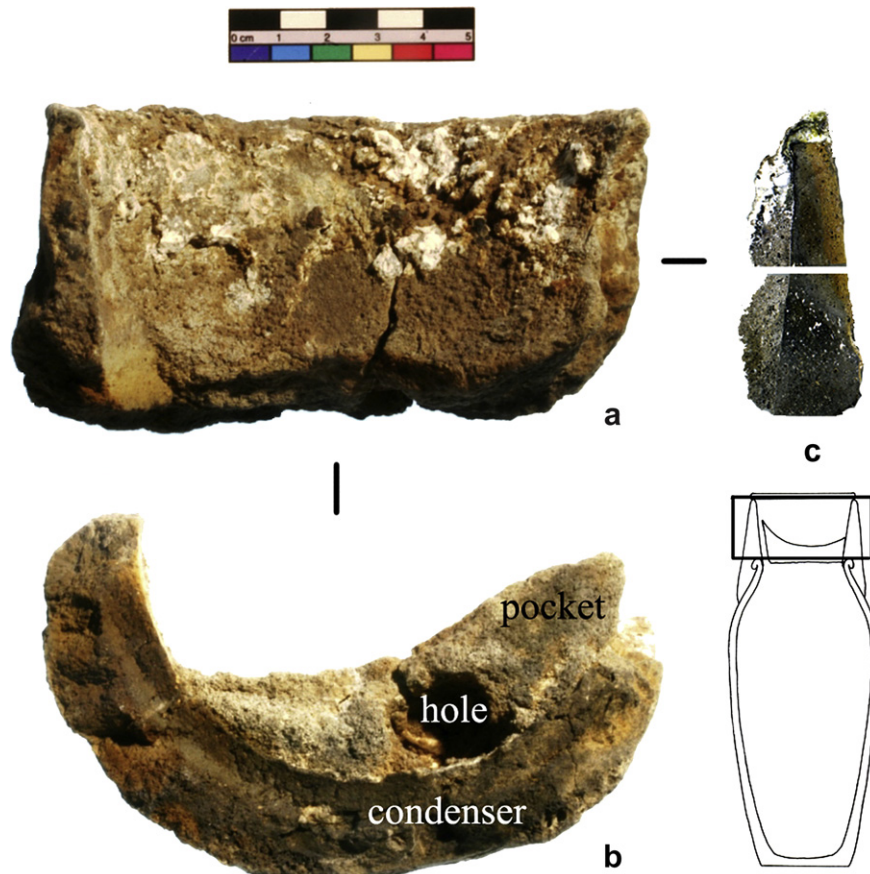


Fig. 8. A condenser fragment YMT1 with part of the pocket and white deposits. (a) internal surface of the condenser; (b) bottom view; (c) vertical cross section.

Table 4

Average bulk compositions of condenser samples from three sites (wt%), normalised to 100%. Analyses on polished sections at areas of ~2 by ~2.5 mm by SEM-EDS. The bottom half rows show the same results after omitting ZnO and renormalising to 100%. “–” means “not detected”.

Site	Sample	MgO	Al ₂ O ₃	SiO ₂	P ₂ O ₅	SO ₃	Cl	K ₂ O	CaO	TiO ₂	MnO	FeO	ZnO
Miaobeihou	YMT1	1.3	12.3	46.1	0.2	0.3	0.1	2.9	2.0	0.5	0.1	5.8	28.4
	YMT3	1.4	14.4	57.7	0.2	0.1	0.3	2.3	2.2	0.8	0.1	7.9	12.6
	YMT8	0.8	9.1	50.8	–	0.1	–	1.6	0.8	0.7	–	4.1	32.0
	YMT12	1.2	13.7	55.8	0.2	0.3	0.1	2.9	0.9	0.8	–	5.7	18.4
	YMT17	1.3	16.5	63.8	0.1	0.1	0.1	2.5	1.9	0.9	0.1	7.0	5.7
	YMT19	1.0	10.2	43.1	0.2	0.6	0.2	1.2	0.9	0.5	0.1	3.7	38.3
	YMT20	0.9	11.5	56.0	0.3	1.1	0.2	4.7	0.9	0.7	0.1	5.0	18.6
	YMT22	1.1	14.5	59.8	0.3	0.2	–	2.1	1.3	0.9	0.1	7.0	12.7
Puzihe	YPT1	1.2	17.0	65.1	0.2	0.2	0.2	1.9	1.1	1.0	0.1	6.9	5.1
	YPT2	0.7	9.1	44.5	0.2	–	0.1	1.3	0.6	0.4	0.0	3.7	39.4
	YPT6	1.1	15.3	64.3	0.3	0.2	0.2	2.4	0.7	0.9	0.1	6.9	7.6
Muxixi	CMT1	1.3	12.4	60.6	0.5	0.3	0.1	2.5	1.8	0.6	0.2	5.1	14.6
	CMT2	1.4	13.0	64.7	0.3	0.1	–	2.9	1.1	0.8	0.1	5.2	10.4
	CMT4	1.5	11.2	60.8	0.2	–	0.2	2.4	0.7	0.7	0.2	5.3	16.8
Miaobeihou	YMT1	1.8	17.2	64.5	0.2	0.4	0.2	4.0	2.7	0.7	0.2	8.1	
	YMT3	1.6	16.5	65.9	0.2	0.1	0.4	2.7	2.5	0.9	0.2	9.0	
	YMT8	1.2	13.4	74.5	–	0.1	0.1	2.4	1.2	1.0	0.1	6.0	
	YMT12	1.5	16.8	68.3	0.2	0.4	0.1	3.6	1.1	1.0	–	7.0	
	YMT17	1.4	17.5	67.6	0.1	0.1	0.1	2.7	2.0	1.0	0.1	7.4	
	YMT19	1.6	16.5	69.9	0.3	1.0	0.3	1.9	1.5	0.8	0.2	6.0	
	YMT20	1.1	14.1	68.8	0.4	1.4	0.2	5.8	1.1	0.9	0.1	6.1	
	YMT22	1.3	16.6	68.6	0.3	0.2	–	2.4	1.5	1.0	0.1	8.0	
Puzihe	YPT1	1.3	17.9	68.5	0.2	0.2	0.2	2.0	1.2	1.1	0.1	7.3	
	YPT2	1.2	14.9	73.3	0.4	0.1	0.1	2.1	0.9	0.7	0.1	6.2	
	YPT6	1.2	16.6	69.6	0.3	0.2	0.2	2.6	0.8	1.0	0.1	7.4	
Muxixi	CMT1	1.5	14.6	70.9	0.6	0.4	0.1	2.9	2.1	0.7	0.2	6.0	
	CMT2	1.6	14.5	72.1	0.4	0.1	–	3.3	1.2	0.9	0.1	5.8	
	CMT4	1.8	13.5	73.2	0.2	–	0.2	2.8	0.8	0.9	0.2	6.4	

generally 2 cm long and 1 cm wide, can be found on one side of pockets, where the thickness of the pockets is larger than the opposite side (Fig. 11). These holes acted as the passage for zinc vapour to rise from the pots to the condensers. The pockets are quite friable and not always recovered. Only four samples from Miaobeihou could be collected for analysis.

The uneven bottom surfaces of the pockets display imprints of the charge below, suggesting that the charges filled the pots to the rims before fresh clay was applied to form the pockets. The bottom surfaces are more vitrified than the upper parts, so they are better preserved. The two samples (YMT2 and YMT8) from the lower parts examined are vitrified, porous with small round bloating pores and larger irregular voids. Their bulk compositions are similar to those

of condensers, with only slightly higher Al₂O₃ and lower SiO₂ contents (Table 5). Like in the condensers, a few large inclusions with layered structures are likely to be coal ash fragments. The main inclusions are quartz grains; a few large ones and higher amounts of semi-molten small ones.

In most cases, the upper parts of pockets are partially missing, perhaps caused by the artisans scraping off zinc rich materials for resmelting after the zinc ingots were collected at the end of the process. The two samples from the upper parts (YMT1 and YMT12) are not vitrified but heavily contaminated by zinc. Large inclusions up to 1 mm in diameter consist of quartz, potassium feldspar and coal ash fragments, while small inclusions are mainly quartz (Fig. 12).

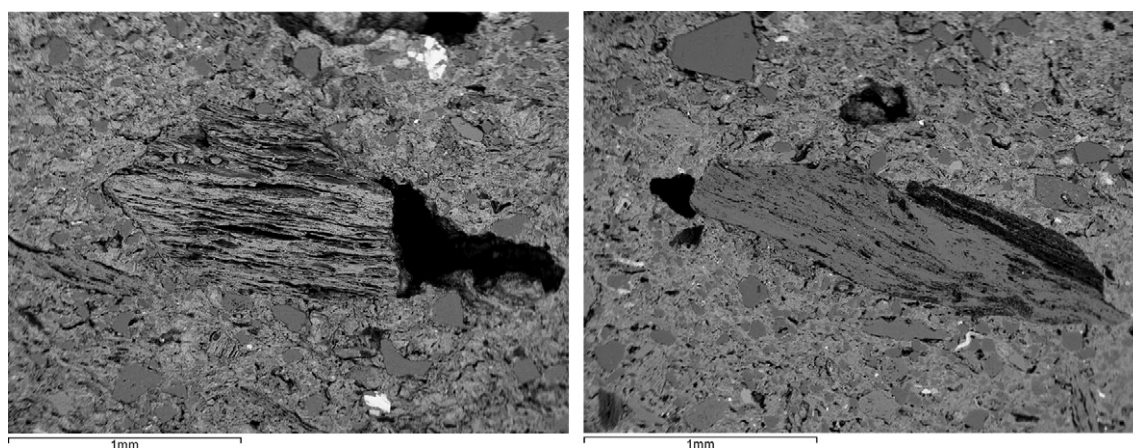


Fig. 9. BSE images of different appearances of coal ash fragments in YMT17. Left: a burnt coal ash fragment; right: a coal ash fragment with a small area rich in carbon (black).

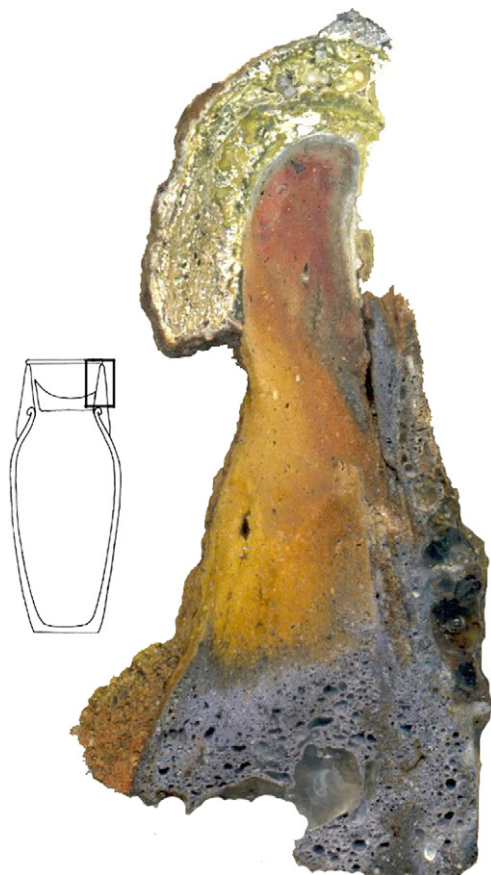


Fig. 10. Cross section of condenser YMT8. The top yellowish and reddish part of the condenser is not vitrified but the lower bluish part is heavily vitrified, which was caused by different temperatures and redox conditions. Note the thick zinc oxide crust adhering to the inner side of the rim and part of pocket fabrics attaching to the internal surface of the condenser. (For interpretation of the references to colour in this figure caption, the reader is referred to the web version of this article).

4.4. Slag

Slag here refers to the metallurgical residues left within the pots after the smelting. The slag is rusty, porous and quite vitrified. The slag is generally adhering to the internal surfaces of the lower parts of pots, and in some cases small fragments of coal and charcoal can still be seen trapped inside the slag (Fig. 13). There are also small discrete lumps of porous and fragile slag found together with retorts at the sites, which indicates that more residues could have formed within the pots. The loose slag was probably removed by the artisans in order to reuse the pots.

The five slag samples from Miaobeihou, two from Puzihe and three from Muxixi contain substantial amounts of SiO_2 (29–58%) and Al_2O_3 (5–15%), which can be partly explained by the contribution of the ceramic to the melt: lumps of ceramic with partly dissolved quartz grains can be frequently identified within the slag. These samples are also rich in FeO, ranging from 10% to the extreme value of 46% in YMB5. They contain variable levels of ZnO (3–15%), CaO (2–10%), MgO (1–4%), BaO (0.2–6%) and SO_3 (0.4–2%) (Table 6). The slag samples are very heterogeneous, which is also manifested in their microstructures. The most common phases in the slag are described below.

Within the glassy phase of slag, a variety of primary phases have crystallised from the silicate melt, including anorthite $\text{CaAl}_2\text{Si}_2\text{O}_8$, celsian $\text{BaAl}_2\text{Si}_2\text{O}_8$, spinel $(\text{Zn},\text{Fe})\text{Al}_2\text{O}_4$, olivine $(\text{Fe}, \text{Mg}, \text{Zn})_2\text{SiO}_4$, pyroxene $(\text{Ca}, \text{Fe}, \text{Mg}, \text{Zn})_2\text{Si}_2\text{O}_6$ and melilite $\text{Ca}_2(\text{Al}, \text{Mg}, \text{Fe})\text{Si}_2\text{O}_7$.

They are generally richer in zinc than the corresponding natural minerals. YMB3 contains a large number of crystals of barite, BaSO_4 , consistent with the higher bulk BaO levels.

Clusters of zinc sulphide and metallic iron are frequent (Fig. 14). Zinc sulphides appear as round globules containing about 6% iron, and as tiny flower-like crystals certainly crystallised from the melt. The metallic iron contains minor amounts of arsenic, zinc, copper and phosphorous. In some areas, iron prills have corroded away, leaving voids where iron oxides are sometimes redeposited. The presence of secondary iron oxides in cracks, pores and surfaces denotes that metallic iron was originally more abundant than apparent today. In YMB5, calcium carbonates are also deposited in the pores, resulting in the high CaO level.

In addition, residues of coal fragments are identified in most slag samples (Fig. 15), as well as some relicts of charcoal fragments that can be clearly recognised through their cell structures in YMB1, YMB2, YMB3 and YPB1 (Fig. 16). This indicates that both mineral and vegetal carbon were part of the charge.

A few residual inclusions of zinc silicates (2–3 mm large) are found in CMM1 and CMB1 (Fig. 17). Sometimes they appear to have recrystallised internally as angular, cored crystals with lower FeO levels in the cores and higher FeO levels (up to 10%) towards their surfaces. However, these inclusions still retain the shapes of original minerals with cracks throughout them. It is likely that zinc silicate crystals from the ores partially melted into the slag and later recrystallised internally to these iron-bearing zinc silicates. Their presence here suggests that zinc silicate minerals, such as those identified in archaeological minerals from Miaobeihou, could not be reduced to metal as easily as zinc oxides or carbonates, which probably explains the higher ZnO contents in these samples.

In CMB1, metallic iron prills, zinc oxides with ~15% of FeO and zinc-rich spinels are embedded within a cluster of iron-bearing zinc silicate crystals (12% FeO). Furthermore, a lump of pure zinc oxide (~500 μm in diameter) is identified with tiny zinc silicate crystals growing between it and the slag melt (Fig. 17). The presence of zinc oxides and the absence of residual coal/charcoal suggest that perhaps in this case there was not enough reducing agent for the complete reduction of zinc oxides.

5. Discussion

The extreme volatility of metallic zinc meant that sophisticated installations were required to reduce it and collect it from its ores. Based on the analytical work, the next sections will present a reconstruction of how this process was put in practice in Fengdu during the Ming period, as well as an explanation of how the formal and material properties of the installation were optimised to meet the required performance characteristics, before turning to a broader contextualisation.

5.1. The distillation reactions

The metallurgical process taking place within the retorts involved two steps: the reduction of zinc ores in the lower reaction zone and the condensation of zinc vapour in the upper condensation zone (Fig. 3).

The analytical results of the slag samples indicate that the charge was composed of zinc ore, coal and charcoal. Most of SiO_2 and Al_2O_3 in the slag were contributed by the pot fabrics as indicated by the strong interaction interface between the slag and the ceramic and their similar ratios of $\text{SiO}_2:\text{Al}_2\text{O}_3$. Crushed condenser walls and pockets were probably added to the charge to recover the zinc contained in them, thereby introducing further SiO_2 and Al_2O_3 . Part of the SiO_2 and Al_2O_3 could also come from the ores and coal ash. The high amounts of FeO and ZnO should derive from ores,

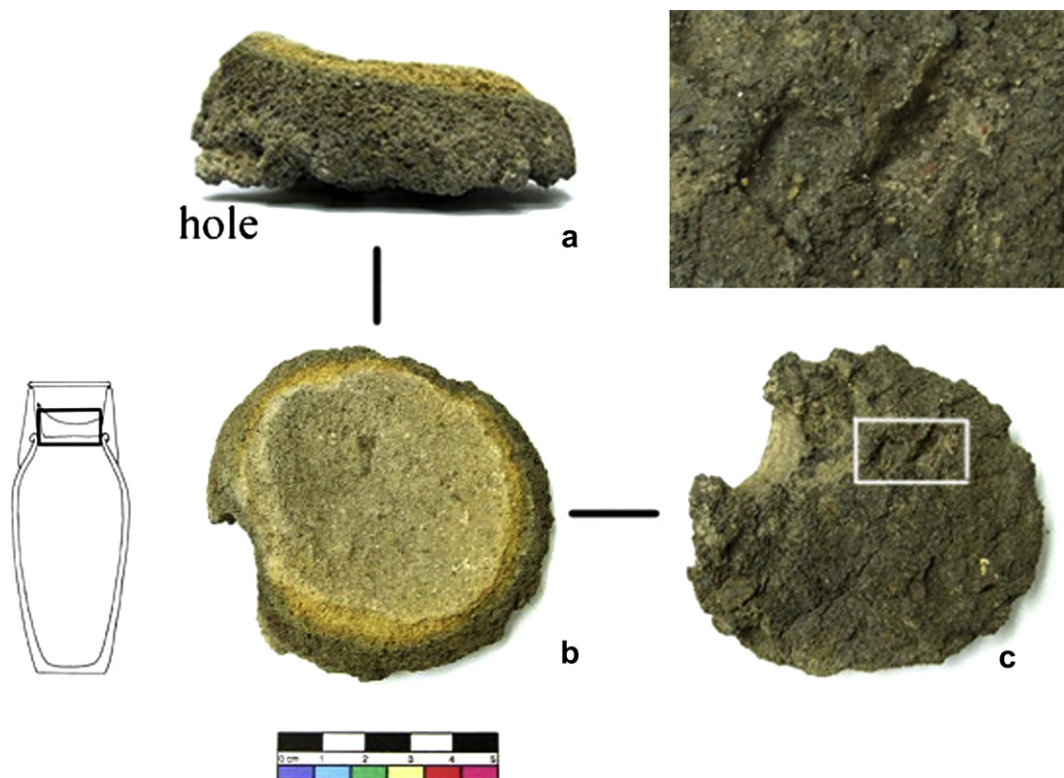


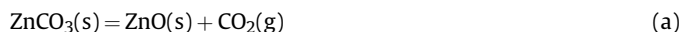
Fig. 11. A pocket from Miaobeihou. (a) side view showing that the side with the hole is thicker; (b) the upper surface; (c) the bottom surface showing clear imprints of the charge with enlarged detail shown above.

which are iron-rich oxidic zinc ores like the iron-rich mineral samples from Miaobeihou discussed above. The elevated levels of CaO, MgO and BaO and SO₃ might originate from the gangue of zinc ores, i.e. calcite, dolomite and barite. In addition, coal and charcoal ash introduced small amounts of CaO, MgO, FeO, SO₃ and P₂O₅ into the slag.

According to the studies of slag and mineral samples from these sites, the zinc ores used were mostly zinc carbonates, smithsonite. Zinc silicates, hemimorphite, could be present in the ores, but they are not easily reduced as zinc carbonates, as indicated by their residual presence in CMM1 and CMB1. The oxidic zinc ores could also contain occasional sulphidic minerals such as sphalerite, but sphalerite could not be converted to zinc under the reducing conditions of the process.

There is no evidence of a separate ore roasting stage at the sites studied. It can therefore be hypothesised that in the reaction zone, zinc ores, mainly zinc carbonates, would be first decomposed to

zinc oxide and carbon dioxide at about 300 °C as per the following reaction:



The carbon dioxide from the zinc carbonates could react with carbon from the coal and charcoal to produce carbon monoxide; in addition, initial oxygen present in the pots could also generate carbon monoxide through reaction with the solid carbon provided by charcoal and coal.

Table 5

Average bulk compositions of pocket samples from Miaobeihou site (wt%), normalised to 100%. Analyses on polished sections at areas of ~2 by ~2.5 mm by SEM-EDS. The bottom half rows show the same results after omitting ZnO and renormalising to 100%.

Sample	MgO	Al ₂ O ₃	SiO ₂	P ₂ O ₅	SO ₃	Cl	K ₂ O	CaO	TiO ₂	FeO	ZnO
YMT2	1.5	18.8	63.1	0.2	0.3	0.3	2.9	2.4	1.0	7.6	1.9
YMT8	1.6	18.0	60.2	0.2	0.3	0.6	4.6	1.9	1.0	5.0	6.6
YMT1	1.0	12.0	34.2	0.3	0.3	0.1	0.9	1.6	0.5	3.4	45.7
YMT12	0.7	7.2	25.3	0.3	1.1	0.2	0.6	0.4	0.2	1.7	62.3
YMT2	1.5	19.2	64.4	0.2	0.3	0.3	3.0	2.4	1.0	7.7	
YMT8	1.8	19.3	64.2	0.2	0.3	0.7	4.9	2.1	1.1	5.4	
YMT1	1.8	22.1	63.0	0.5	0.6	0.2	1.7	3.0	0.9	6.2	
YMT12	1.8	19.2	67.0	0.7	3.0	0.6	1.5	1.2	0.6	4.4	

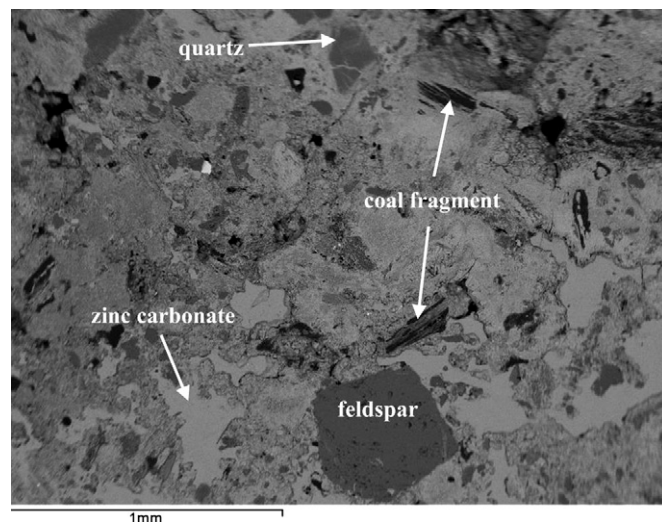
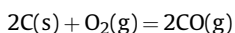
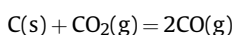


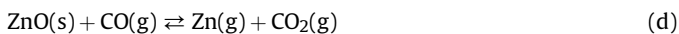
Fig. 12. BSE image of the cross section of pocket YMT1, showing quartz, feldspar, coal ash fragments and zinc carbonates.



Fig. 13. Slag adhering to the bottom of pot YMB1.



As the temperature reached over 1000 °C, zinc oxide was reduced to the metallic state by carbon monoxide. The carbon dioxide released could produce more carbon monoxide by reacting with coal and charcoal, thus keeping the reversible reaction to the right.



Generally an excess of carbon was required to reduce zinc oxide, as confirmed by the unreacted coal and charcoal residues identified in most of the slag; while insufficient carbon would leave

unreduced zinc oxides, as identified in sample CMB1. A temperature of ~1200 °C was generally achieved in the reaction zone, as estimated by the temperature-induced mineral transformations and the degree of vitrification of the pots. Highly reducing conditions were kept during the process, as indicated by iron prills and zinc sulphide forming in the slag.

The zinc produced, in the form of vapour, ascended via the hole of the pocket to the condensation zone. Zinc vapour was liquified first below its boiling point of 907 °C when it reached the cooler lids and walls of condensers and dripped into the pockets. The zinc droplets trapped in the zinc oxide crusts at the upper parts of the condensers confirm that zinc was in a liquid state before solidification below its melting point of 420 °C. There was a significant temperature drop just above the mouth of pots, as seen from the lower degree of vitrification of condensers and pockets. A reducing

Table 6
Bulk compositions (top half) and glassy matrix (bottom half) of slag samples from three sites (wt%), normalised to 100%. Analyses on polished sections at areas of ~2 by ~2.5 mm and ~400 by ~600 μm respectively by SEM-EDS. “–” means “not detected”.

Site	Sample	MgO	Al ₂ O ₃	SiO ₂	P ₂ O ₅	SO ₃	Cl	K ₂ O	CaO	TiO ₂	MnO	FeO	CuO	ZnO	BaO	PbO
Miaobeihou	YMB1	3.5	10.4	44.6	0.3	2.3	0.2	1.4	5.3	0.5	0.1	20.7	0.1	8.8	1.8	–
	YMB2	2.3	12.6	53.6	0.2	1.1	0.2	2.3	4.5	0.7	0.2	11.4	0.1	8.4	2.4	–
	YMB3	1.8	8.3	31.7	0.2	2.1	0.3	1.0	3.2	0.4	0.3	42.3	0.2	2.6	5.5	0.1
	YMB4	2.3	10.8	53.4	0.1	1.6	0.3	1.8	5.2	0.7	0.1	11.9	0.1	9.6	2.0	0.1
	YMB5	4.0	5.6	28.8	0.4	0.5	0.2	0.3	9.7	0.2	0.2	45.8	–	4.1	0.2	–
Puzihe	YPB1	1.3	15.3	58.2	0.3	0.4	0.3	3.4	2.1	0.8	0.1	9.7	0.1	6.8	1.2	–
	YPB5	3.3	13.1	41.3	0.2	0.6	0.1	1.0	7.5	0.6	0.1	28.6	0.2	3.1	0.3	–
Muxixi	CMM1	3.8	7.3	33.1	0.2	0.8	0.2	0.5	5.1	0.3	0.2	32.8	0.1	14.3	1.3	–
	CMB1	3.0	9.1	45.8	0.3	1.4	0.1	1.4	5.3	0.3	0.2	15.6	0.1	15.2	2.1	0.1
	CMB4	2.3	12.1	57.9	0.2	0.6	0.1	1.8	3.5	0.4	0.2	15.6	0.1	3.4	1.8	–
Miaobeihou	YMB1	3.0	12.0	51.9	0.1	0.8	0.1	1.8	5.7	0.7	0.2	13.7	–	8.3	1.7	–
	YMB2	2.6	12.8	55.9	0.1	0.5	–	2.3	5.0	0.8	0.2	9.2	–	8.2	2.4	–
	YMB3	2.5	12.5	57.2	0.2	0.3	0.1	2.4	6.6	0.7	0.4	8.2	–	5.5	3.4	–
	YMB4	3.0	10.5	54.1	0.1	0.9	0.2	2.0	5.7	0.6	0.2	10.8	–	9.8	2.1	–
	YMB5	4.8	8.8	49.3	0.4	1.0	0.3	0.8	12.8	0.4	0.4	14.0	–	6.6	0.4	–
Puzihe	YPB1	1.7	16.3	59.8	0.2	0.3	0.2	3.9	2.6	1.0	0.2	5.1	–	7.8	0.8	0.1
	YPB5	3.7	16.6	58.1	0.2	0.5	0.1	2.2	10.0	0.9	0.2	4.0	0.1	3.1	0.3	–
Muxixi	CMM1	5.8	9.2	42.8	0.2	1.1	0.3	0.9	7.0	0.4	0.2	15.0	–	15.4	1.6	0.1
	CMB1	3.0	9.7	51.3	0.3	0.8	0.1	1.7	5.7	0.5	0.2	10.0	–	14.2	2.5	–
	CMB4	2.7	13.2	58.9	0.1	0.5	0.1	1.9	3.9	0.6	0.3	12.3	–	3.6	1.9	–

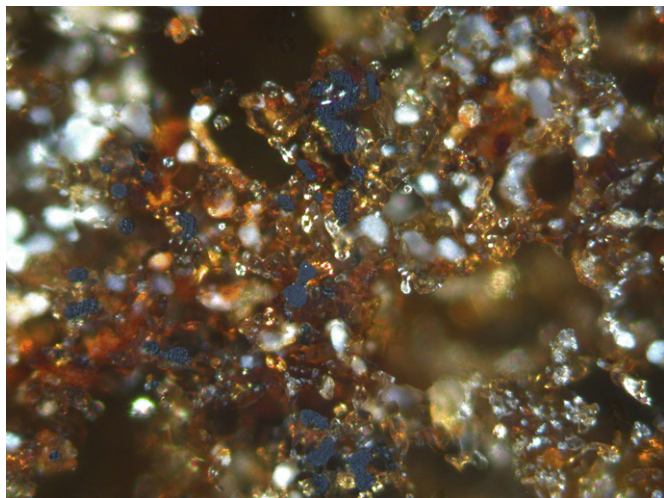


Fig. 14. XPL image of the cross section of slag YMB2, showing zinc sulphide (yellow), metallic iron (dark) and voids (white), width of picture 0.5 mm. (For interpretation of the references to colour in this figure caption, the reader is referred to the web version of this article).

atmosphere was required to prevent the oxidation of zinc, but it was inevitable that some zinc was oxidised, forming the zinc-rich crusts documented in some condensers and pockets – which could be recycled –, and also being lost in the fumes.

The planoconvex cake ingots found at Miaobeihou in the 1980s strongly indicate that the newly formed metallic zinc solidified within the concave depressions of the pockets rather than being poured while liquid. These cakes were oval because of the shapes of the pocket depressions – the sides with holes being higher (Fig. 3). Although we have been unable to examine these ingots directly, their descriptions and dimensions seem to fit the pockets well. They were possibly remelted and cast into larger ingots like the rectangular ones (Fig. 4). The raw zinc produced was of high purity, with involatile materials left in the slag and lead being the only impurity in the metal. Although only traces of PbO were detected in mineral and slag samples, zinc ores richer in lead can be assumed to have been used to produce the zinc metal with half a percent lead

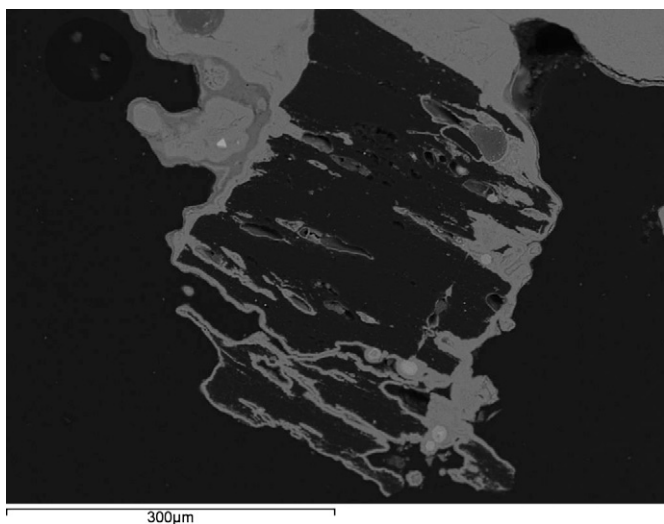


Fig. 15. BSE image of the cross section of slag YMB1, showing the coal fragment (black, middle) and rusts (grey).

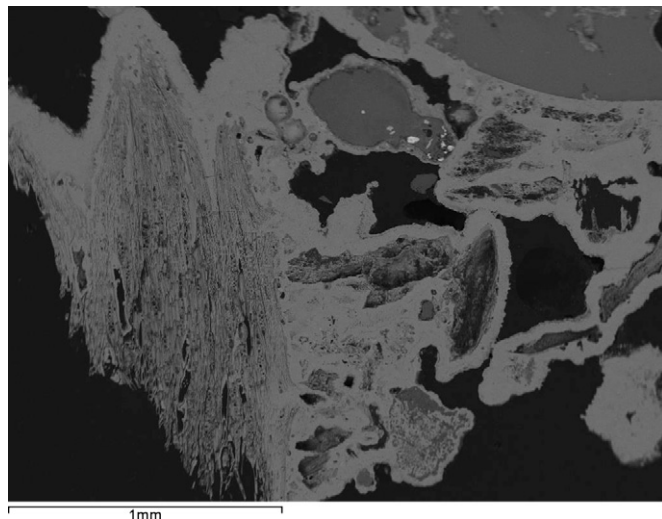


Fig. 16. BSE image of the cross section of slag YMB1, showing the relicts of charcoal.

documented here. The zinc ores used were rich in iron, but only traces of iron entered the metal with most of it staying in the slag.

The capacity of an ordinary Miaobeihou retort is estimated to be about 2 L, roughly calculated from a cylinder with an internal diameter of 10 cm and a height of 26 cm. Assuming the charge consisted of zinc ores with a grade of 35% ZnO and an excess of coal as high as three times the theoretical value (based on Hopkins, 1954, 187), the volume ratio of ore to coal was about 2:1, using specific gravities of 2.5 for ores and 0.8 for coal. Given no loss of zinc, the zinc metal produced per retort was about 0.9 kg. If the reducing agent was charcoal alone (specific gravity 0.5), 0.8 kg zinc could be produced per retort. Allowing for some zinc loss, an ordinary retort could therefore produce 0.6–0.7 kg of metallic zinc per firing, roughly corresponding to the weight of the planoconvex ingots described above.

5.2. Retort design

The different parts of retorts all exhibit appropriate formal and material properties suitable for their specific performance characteristics.

The pots have the shape of ordinary storage jars, thus having a large capacity to retain the charge. The similarities among pots from three sites in terms of shape, size, material (clay and quartz temper) and manufacturing technology suggest that there were specialised pottery workshops and kilns to make them, possibly near these zinc workshops. They are stable on their flat bottoms. The whole or part of bases of used retorts show fewer firing traces, indicating that the pots were sitting on the furnace bars in the cases of rectangular furnaces. The increasing wall thickness of jars from the top to the bottom would not only maintain structural stability, but also provide enough strength to retain the charge. It would also enhance the resistance to the chemical attack by the reacting charge at the bottom parts. The clay used for the pots was quite refractory, with about 21% Al₂O₃, but not of the highly refractory fireclay type, as indicated by its relatively high FeO and K₂O levels. The addition of quartz improved their physical and thermal properties, as has been demonstrated by mechanical tests on ceramics tempered with sand (Kilikoglou et al., 1998; Tite et al., 2001). The cracks and pores developed in the clay-quartz system can arrest and stop crack propagation under mechanical and thermal stresses, therefore increasing the toughness and thermal shock resistance of these pots. In addition, the pots were fired at a high temperature of

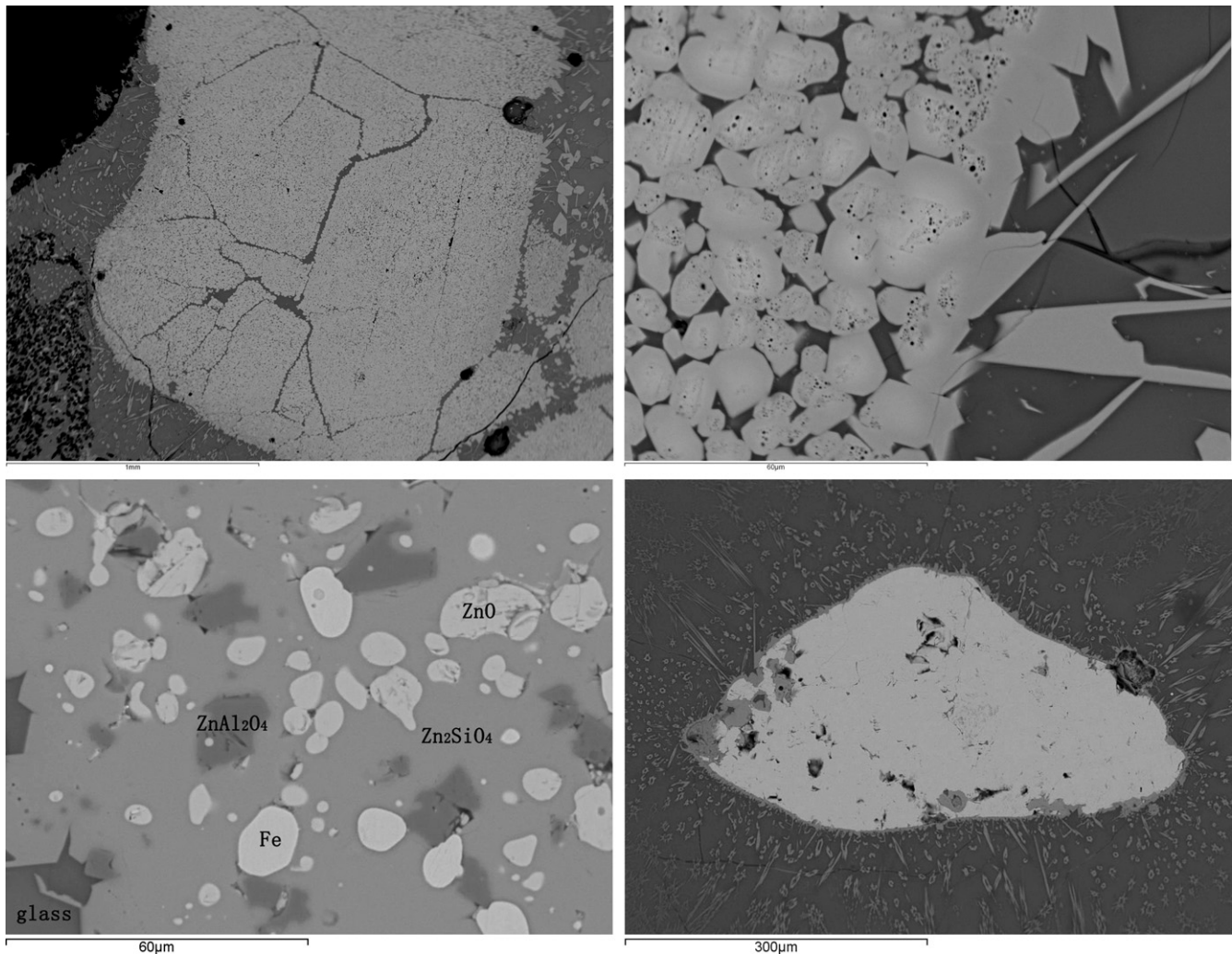


Fig. 17. BSE images of the cross sections of CMM1 and CMB1. Top left: an inclusion of zinc silicate in CMM1; top right: enlarged detail of zinc silicate inclusion in CMM1; bottom left: metallic iron prills (Fe), zinc oxides (ZnO) with ~15% of FeO and zinc-rich spinel (ZnAl_2O_4), in iron-bearing zinc silicates (Zn_2SiO_4) with 12% FeO in CMB1; bottom right: a lump of zinc oxide in CMB1.

about 1200 °C before being used for smelting. This pre-firing produced extensively vitrified fabrics with closed porosity which were more resistant to the corrosive attack of the charge, and limited the penetration of zinc vapour formed during smelting: it is noteworthy that ZnO levels in the pot fabrics rarely exceed 1% in spite of the high pressure of zinc vapour that must have developed during the reaction. Similar clays tempered with quartz were used for making crucibles for brass cementation in Zwickau, Germany, in the late 15th century, but the crucible fabrics were contaminated by 7–8% ZnO, probably due to lower pre-firing temperatures (Martín-Torres and Rehren, 2002). Pots could have been reused after removing pockets, condensers and slag.

The condensers, hand-built with a different clay tempered with coal ash, were probably added to the pots at each smelting workshop. The condensers have thicker walls in the lower parts than the top parts, which not only contributed to structural stability, but also acted – together with the pockets – as a thick insulating barrier to contain the strong heat below the rims of pots. Compared to the pots, the condensers are made of less refractory clays with higher levels of alkali and alkaline earth elements and iron oxide. It was not necessary for condensers to be refractory as they were exposed to much lower temperatures (<800 °C) than the pots (~1200 °C) during the process. They were probably not pre-fired prior to

smelting. The choice of coal ash fragments as temper for condensers might be due to two reasons. On the one hand, coal ash fragments could have contributed to the mechanical properties of the condensers like other platy or fibrous inclusions (such as mica and shell), which are effective at stopping crack propagation, thus increasing both toughness and thermal shock resistance (Tite et al., 2001). On the other hand, it should be noted that coal ash was produced in abundance in zinc smelting furnaces. If it was not recycled, it would have to be dumped as waste. Thus the use of coal ash as temper in the condensers was probably out of practical considerations too.

The thick pockets with concave upper surfaces served as containers for collecting zinc and as insulating barriers from the strong heat in the reaction zone. The pocket fabrics were also less refractory than the pots but similar to the condensers. However, the fabrics are not compressed as tightly as pots and condensers, as shown by the porous vitrified lower parts and the upper parts which are heavily contaminated by zinc. Similarly to the condensers, the pockets would not need to be exposed to high temperatures, so the less refractory fabrics would be sufficient; they were not pre-fired before use.

Finally, the top openings of condensers must have been closed by lids. Small holes should have been present in the lids, opposite the

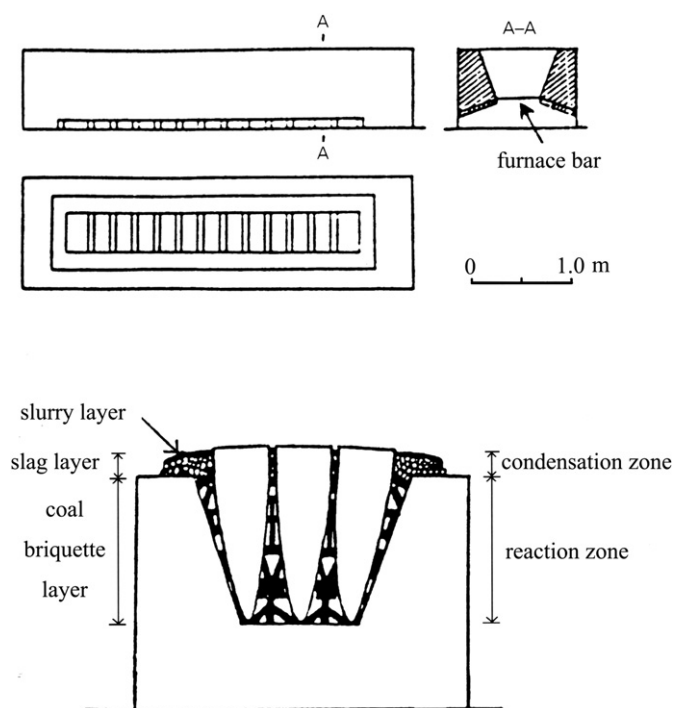


Fig. 18. Trough-shaped furnaces used in Guizhou, southwest China in 1980s (Xu, 1998).

holes of the pockets, so that the gases generated by the process could escape. At Miaobeihou, no lids have been found except a possible one – an iron fragment, 0.4 mm thick. A few round iron lids have been found in Fengdu. A heavily corroded iron lid, 11.6 cm in diameter and 0.8 cm thick, was found at Zhangjiahe site near Miaobeihou (Hunan Provincial Archaeology Institute et al., 2007). More iron lids were also discovered at Dafengmen site in neighbouring Shizhu county during field survey in 2005. As iron has good thermal conductivity, lids made of iron could transfer heat fast into the air and keep the condensation zone at adequate temperatures for condensation. In addition, iron lids could be reused many times, which would also explain their general scarcity in the archaeological record.

The furnaces were of the rectangular type, which continued to be used by the traditional process until the end of last century (Xu, 1998) (Fig. 18). In rectangular furnaces, retorts were placed on furnace bars; each furnace bar generally accommodated 3 retorts. If a furnace bar held 3 retorts, as was the case in the trough furnaces used in the traditional process, then a furnace with 60 furnace bars, like Y2 at Puzihe, could accommodate 180 retorts. Even if one retort only produced less than 1 kg of zinc, one furnace with 180 retorts could produce over 100 kg of zinc per firing.

The temperature control between the two chambers of the retorts was a key issue for successful zinc distillation. From the coal ash fragments visible on the external surfaces of the pots, it is inferred that coal was placed surrounding the pots. As documented in ethnographic examples (Hu and Han, 1984; Xu, 1998; Zhou, 1996; Craddock and Zhou, 2003), coal briquettes, made of coal powder and clay, may have been used. The clay binds coal together and its sintering makes coal briquettes strong enough to support the retorts and upper coal briquettes. Such coal briquettes could burn all day long without forced draught. The spaces between each pair of furnace bars acted as air passages to provide air for the combustion. No heat was supplied around the condensers, so the external surfaces of condensers are not vitrified. There is no clear evidence as to how the steep temperature drop was managed. In the traditional process, this was achieved by sealing the space

between the top parts of retorts with slag and slurry to keep the heat beneath (Xu, 1998).

5.3. Broader contextualisation

Lacking detailed information about site dimensions and relative chronologies, it is difficult to estimate the amount of zinc produced in Fengdu during the Ming period. Although it is possible that retorts would be reused when the slag could be detached from the inside, the uncertainty about this point makes it even harder to gauge the yield of the site even by counting the number of pots preserved. There is no doubt, in any case, that the scale of production must have been impressive, since about 20 sites have hitherto been excavated by the river, including a total of over 20 furnace foundations, and thousands of retorts litter the area. It is therefore surprising that no historical records have been found recording the mass production of zinc in this region and period. Zinc production at this scale must have consumed vast amounts of raw materials, especially zinc ores and coal, and it is likely that it supplied a governmental consumer.

The nearest zinc ore deposits are the Laochangping lead-zinc deposits in Shizhu, about 50 km to the southeast from the zinc smelting sites by the river. There is a long history of mining and smelting of copper, lead and silver in the mountainous Laochangping region since the Tang Dynasty (AD 618–907). Zinc ores had been exploited at least since the late Ming Dynasty. Inside an old mine named Yushi Cave, a geologist reported seeing a stela with inscriptions recording the opening ceremony for mining the cave in 1576 (Wang, 1991), i.e. contemporary with the mass production of zinc in Fengdu. The ores exploited in the cave are visually similar to the mineral fragments discovered at Miaobeihou. Therefore, it is most likely that the zinc smelting sites in Fengdu used ores from Shizhu. These ores could be transported via the Dragon River to the Yangtze River (Fig. 1).

Besides zinc ores, a great amount of coal was needed for zinc smelting, as it was used both as a reducing agent inside retorts and as fuel outside them. In ancient China, coal was widely used in everyday life and crafts, for example in iron smelting since the Song dynasties (AD 960–1279). A few coal deposits are known in Fengdu, which could have been exploited by the zinc smelters during the Ming period. In addition, coal could also be transported from other areas via the Yangtze River.

Although there are no direct historical documents recording Fengdu zinc industry in that period, it is known that, in the late Ming Dynasty, zinc was mostly used to make brass coins, which were cast in the central mint in the capital Beijing as well as provincial mints in most provinces. The large-scale production of zinc in Fengdu was probably set up to supply alloying materials for minting. The location of these sites by the river, rather than in closer proximity to the mines, may have been driven by the government's desire to control production. Furthermore, the Yangtze River would provide a convenient means to ship the zinc ingots produced to the mints.

6. Conclusion

The analyses of metallurgical remains from three zinc smelting sites in Fengdu have allowed for the first time a detailed reconstruction of zinc smelting technology based on production remains from the Ming period. These zinc workshops used similar retorts composed of pots, condensers, pockets and lids, all of them well designed to meet different performance characteristics. Oxidic zinc ores were reduced to zinc vapour with coal and charcoal within the pots under high temperatures of about 1200 °C and strongly reducing conditions; the zinc vapour formed passed through the holes of the pockets and condensed in the cooler condensation area. Firing a great number of retorts in rectangular furnaces at one time

allowed the production of high-purity zinc on a very large scale, probably to supply governmental mints. More work could be carried out on the organisation of production and the distribution of the products.

The sites in Fengdu are the earliest archaeological evidence of zinc production in China to date, consistent with the indirect evidence from historical documents and brass coins. Zinc production technology should have taken a long period to evolve to the advanced technology and large scale in Fengdu. How and why zinc distillation processes originated and evolved in ancient China is still an important issue to be explored, waiting for more archaeological evidence in the future.

Recent field survey has revealed a multiplicity of metallurgical operations that took place in Shizhu, i.e. further from the Yangtze River and closer to the Laochangping lead-zinc mine. There were large amounts of tap slag from lead and copper smelting (Xie and Rehren, 2009), but also zinc smelting retorts appearing externally different from those in Fengdu, which are the subject of ongoing analyses. It is hoped that these detailed studies will allow us to progressively map the spatial and temporal variability of zinc smelting technologies, considering how they were adapted to different social and natural environments and specific political constraints.

Acknowledgements

This work is part of doctoral research by the first author at the Institute of Archaeology, University College London, funded by a Kwok Foundation scholarship (2008–2011). It is also supported by the research project *Multidisciplinary Study of Zinc Smelting Sites in Fengdu*, Chongqing of the State Administration of Cultural Heritage of China. We are very grateful to Director Zou Houxi and Vice Director Yuan Dongshan from Chongqing Municipal Bureau of Cultural Heritage, Director Li Guohong from Fengdu County Bureau of Cultural Heritage, and Professor Wu Xiaohong from Peking University. Special thanks are given to Thilo Rehren and Paul Craddock for their invaluable advice and comments, and to Kevin Reeves, Philip Connolly and Simon Groom for technical support.

References

- Bayley, J., 1984. Roman brass-making in Britain. *Historical Metallurgy* 18 (1), 42–43.
- Bayley, J., 1998. The production of brass in antiquity with particular reference to Roman Britain. In: Craddock, P.T. (Ed.), *2000 Years of Zinc and Brass*, second ed. British Museum Press, London, pp. 7–26.
- Bonin, A., 1924. *Tutenag and Pakong*. Oxford University Press, Oxford.
- Bowman, S., Cowell, M., Cribb, J., 1989. Two thousand years of coinage in China: an analytical survey. *Historical Metallurgy* 23 (1), 25–30.
- Cowell, M., Cribb, J., Bowman, S., Shashoua, Y., 1993. The Chinese cash: composition and production. In: Archibald, M.M., Cowell, M.R. (Eds.), *Metallurgy in Numismatics*, vol. 3. Royal Numismatic Society, London, pp. 185–196.
- Craddock, P.T., Freestone, I.C., Gurjar, L.K., Middleton, A.P., Willies, L., 1998. Zinc in India. In: Craddock, P.T. (Ed.), *2000 Years of Zinc and Brass*, second ed. British Museum Press, London, pp. 27–72.
- Craddock, P.T., Hook, D.R., 1997. The British Museum collection of metal ingots from dated wrecks. In: Redknap, M. (Ed.), *Artefacts from Wrecks: Dated Assemblages from the Late Middle Ages to the Industrial Revolution*. Oxbow Books, Oxford, pp. 143–154.
- Craddock, P.T., Zhou, W., 2003. Traditional zinc production in modern China: survival and evolution. In: Craddock, P.T., Lang, J. (Eds.), *Mining and Metal Production throughout the Ages*. British Museum Press, London, pp. 267–292.
- Dai, Z., Zhou, W., 1992. Studies of the alloy composition of more than two thousand years of Chinese coins (5th century B.C.–20th century A.D.). *Historical Metallurgy* 26 (1), 45–55.
- Day, J., 1998. Brass and zinc in Europe from the Middle Ages until the mid-nineteenth century. In: Craddock, P.T. (Ed.), *2000 Years of Zinc and Brass*, second ed. British Museum Press, London, pp. 133–158.
- de Ruelle, M., 1995. From *conterfei* and *speauter* to zinc: the development of the understanding of the nature of zinc and brass in post-Medieval Europe. In: Hook, D.R., Gaimster, D.R.M. (Eds.), *Trade and Discovery: The Scientific Study of Artefacts from Post-Medieval Europe and Beyond*. British Museum Press, London, pp. 195–203.
- Dungworth, D., White, H., 2007. Scientific examination of remains from Warmley, Bristol. *Historical Metallurgy* 41 (1), 77–83.
- Hopkins, D.W., 1954. *Physical Chemistry and Metal Extraction*. Garnet Miller, London.
- Hu, W., Han, R., 1984. Ancient Chinese zinc smelting technology seen from traditional zinc smelting. *Chemistry* 7, 59–61. 胡文龙 韩汝芬: 从传统法炼锌看我国古代炼锌技术. 《化学通报》7期, 1984年.
- Hunan Provincial Archaeology Institute, Changsha Civic Archaeology Institute, Chongqing Municipal Bureau of Cultural Heritage, Fengdu County Bureau of Cultural Heritage, 2007. Report on Zhangjiahe site in Fengdu. In: Chongqing Municipal Bureau of Cultural Heritage, Chongqing Municipal Bureau of Immigration (Eds.), *Archaeological Reports of Chongqing Reservoir in 2001*. Science Press, Beijing, pp. 1698–1704. 湖南省文物考古研究所 长沙市文物考古研究所 重庆市文物局 丰都县文物管理局: 丰都张家河遗址发掘简报. 重庆市文物局 重庆市移民局 编: 《重庆库区考古报告集 2001年卷》, 科学出版社, 2007年.
- Kilikoglou, V., Vekinis, G., Maniatis, Y., Day, P.M., 1998. Mechanical performance of quartz-tempered ceramics: part I, strength and toughness. *Archaeometry* 40 (2), 261–279.
- Liu, H., Chen, J., Li, Y., Bao, W., Wu, X., Han, R., Sun, S., Yuan, D., 2007. Preliminary multidisciplinary study of the Miaobeihou zinc-smelting ruins at Yangliusi village, Fengdu county, Chongqing. In: Niece, S.L., Hook, D.R., Craddock, P.T. (Eds.), *Metals and Mines: Studies in Archaeometallurgy*. Archetype, London, pp. 170–177.
- Maniatis, Y., Tite, M.S., 1981. Technological examination of Neolithic-Bronze Age pottery from central and southeast Europe and from the Near East. *Journal of Archaeological Science* 8, 59–76.
- Martinón-Torres, M., Freestone, I.C., Hunt, A., Rehren, Th., 2008. Mass-produced mullite crucibles in medieval Europe: manufacture and material properties. *Journal of American Ceramic Society* 91 (6), 2071–2074.
- Martinón-Torres, M., Rehren, Th., 2002. Agricola and Zwickau: theory and practice of Renaissance brass production in SE Germany. *Historical Metallurgy* 36 (2), 95–111.
- Mei, J., 1990. Modern Chinese traditional zinc smelting. *China Historical Materials of Science and Technology* 11 (2), 33–37. 梅建军: 近代中国传统炼锌术. 《中国科技史料》11卷2期, 1990年.
- Ohya, Y., Takahashi, Y., Murata, M., Nakagawa, Z., Hamano, K., 1999. Acoustic emission from a porcelain body during cooling. *Journal of American Ceramic Society* 82 (2), 445–448.
- Rehren, Th., 1999a. “The same...but different”: a juxtaposition of Roman and medieval brass making in central Europe. In: Young, S.M.M., Pollard, A.M., Budd, P., Ixer, R.A. (Eds.), *Metals in Antiquity*. Archaeopress, Oxford, pp. 252–257.
- Rehren, Th., 1999b. Small size, large scale: Roman brass making in Germania Inferior. *Journal of Archaeological Science* 26 (8), 1083–1087.
- Shanxi Provincial Archaeology Institute, Chongqing Municipal Bureau of Cultural Heritage, 2007. Archaeological report of Puzihe site in Fengdu. In: Chongqing Municipal Bureau of Cultural Heritage, Chongqing Municipal Bureau of Immigration (Eds.), *Archaeological Reports of Chongqing Reservoir in 2001*. Science Press, Beijing, pp. 1705–1770. 山西省考古研究所 重庆市文物局: 丰都铺子河遗址考古发掘报告. 重庆市文物局 重庆市移民局 编: 《重庆库区考古报告集 2001年卷》, 科学出版社, 2007年.
- Souza, G.B., 1991. Ballast goods: Chinese maritime trade in zinc and sugar in the seventeenth and eighteenth centuries. In: Ptak, R., Rothermund, D. (Eds.), *Emporia, Commodities and Entrepreneurs in Asian Maritime Trade, c.1400–1750*. Steiner Verlag, Stuttgart, pp. 291–315.
- Tite, M.S., Kilikoglou, V., Vekinis, G., 2001. Review article: strength, toughness and thermal shock resistance of ancient ceramics, and their influence on technological choice. *Archaeometry* 43 (3), 301–324.
- Tite, M.S., Maniatis, Y., Meeks, N.D., Binson, M., Hughes, M.J., Leppard, S.C., 1982. Technological studies of ancient ceramics from the Near East, Aegean and Southeast Europe. In: Wertime, T.A., Wertime, S.F. (Eds.), *Early Pyrotechnology: the Evolution of the First Fire-using Industries*. Smithsonian Institution Press, Washington, DC, pp. 61–71.
- Wang, W., 1991. Visit to Laochangping mining cave. *Historical Accounts of Shizhu* 13, 51–54. 王方知: 老厂坪矿洞见闻. 《石柱文史资料》13辑, 1991年.
- Wolf, S., 2002. Estimation of the production parameters of very large medieval bricks from St. Urban, Switzerland. *Archaeometry* 44 (1), 37–65.
- Xie, P., Rehren, Th., 2009. Scientific analysis of lead-silver smelting slag from two sites in China. In: Mei, J., Rehren, Th. (Eds.), *Metallurgy and Civilisation: Eurasia and Beyond*. Archetype, London, pp. 177–183.
- Xu, L., 1998. Traditional zinc-smelting technology in the Guma district of Hezhang County. In: Craddock, P.T. (Ed.), *2000 Years of Zinc and Brass*, second ed. British Museum Press, London, pp. 115–131.
- Zhang, H., 1925. Further discussion on the origin of the use of zinc in China. *Science* 9 (9), 1116–1127. 章鸿钊: 再述中国用锌之起源. 《科学》9卷9期, 1925年.
- Zhao, K., 1984. Further discussion on the origin of zinc in China. *China Historical Materials of Science and Technology* 5 (4), 15–23. 赵匡华: 再探我国用锌起源. 《中国科技史料》5卷4期, 1984年.
- Zhou, W., 1993. A new study on the history of the use of zinc in China. *Bulletin of the Metals Museum* 19, 49–53.
- Zhou, W., 1996. Chinese traditional zinc-smelting technology and the history of zinc production in China. *Bulletin of the Metals Museum* 25, 36–47.
- Zhou, W., 2001. The emergence and development of brass-smelting techniques in China. *Bulletin of the Metals Museum* 34, 87–98.
- Zhou, W., Fan, X., 1993. A study on the development of brass for coinage in China. *Bulletin of the Metals Museum* 20, 35–45.